OPEN

Citation: Cell Death and Disease (2014) 5, e1054; doi:10.1038/cddis.2014.11

www.nature.com/cddis

Early and sustained altered expression of aging-related genes in young 3xTg-AD mice

V Gatta[1,2,7], M D'Aurora[1,3,7], A Granzotto[4], L Stuppia[1,2] and SL Sensi*[,3,4,5,6]

Alzheimer's disease (AD) is a multifactorial neurological condition associated with a genetic profile that is still not completely understood. In this study, using a whole gene microarray approach, we investigated age-dependent gene expression profile changes occurring in the hippocampus of young and old transgenic AD (3xTg-AD) and wild-type (WT) mice. The aim of the study was to assess similarities between aging- and AD-related modifications of gene expression and investigate possible interactions between the two processes. Global gene expression profiles of hippocampal tissue obtained from 3xTg-AD and WT mice at 3 and 12 months of age (m.o.a.) were analyzed by hierarchical clustering. Interaction among transcripts was then studied with the Ingenuity Pathway Analysis (IPA) software, a tool that discloses functional networks and/or pathways associated with sets of specific genes of interest. Cluster analysis revealed the selective presence of hundreds of upregulated and downregulated transcripts. Functional analysis showed transcript involvement mainly in neuronal death and autophagy, mitochondrial functioning, intracellular calcium homeostasis, inflammatory response, dendritic spine formation, modulation of synaptic functioning, and cognitive decline. Thus, overexpression of AD-related genes (such as mutant *APP*, *PS1*, and hyper-phosphorylated tau, the three genes that characterize our model) appears to favor modifications of additional genes that are involved in AD development and progression. The study also showed overlapping changes in 3xTg-AD at 3 m.o.a. and WT mice at 12 m.o.a., thereby suggesting altered expression of aging-related genes that occurs earlier in 3xTg-AD mice.
Cell Death and Disease (2014) **5,** e1054; doi:10.1038/cddis.2014.11; published online 13 February 2014
Subject Category: Neuroscience

Alzheimer's disease (AD) is the most common form of dementia in the elderly population.[1] According to the 'amyloid cascade' hypothesis, amyloid dysmetabolism and formation of tau-containing neurofibrillary tangles (NFTs) are key steps in the disease.[2] Aging is also a critical factor for sporadic AD and a lively debate on whether the disease is actually driven by aging is animating the field.[3] The 'age-based hypothesis' postulates that initiating injury factors like head trauma, infections, vascular alterations, diabetes, or even genetic mutations, when operating on the aging brain, promote neuroinflammation and initiate the AD-related pathogenic cascade.[2,3] Thus, brain aging along with neuroinflammation are crucial conditions on which pro-AD events must work to successfully initiate the disease.

Genetic aspects of AD have been intensively investigated for decades (see Tanzi[4] for an extensive review on the topic); however, crucial information is still missing to successfully compose the puzzle. Microarray technology allows the simultaneous analysis of thousands of transcripts in a single experiment and is a useful approach for the investigation of a wide range of gene-related diseases. Gene expression studies in transgenic AD models have helped to unravel genetic factors influencing disease progression at well-defined stages as well as their relation with the development of cognitive deficits.[5]

Thus, in the present study we employed a whole genome microarray approach to investigate age-dependent gene expression profile changes in hippocampi obtained from young (3 months of age (m.o.a.)) and old (12 m.o.a.) 3xTg-AD mice. This model offers the selective advantage of combining both amyloid (Aβ)- and tau-dependent pathology and is a largely investigated and more comprehensive preclinical model of AD.[6] To control for age-dependent transcript modifications, we also investigated changes occurring in age-matched wild-type (WT) mice.

In designing our experiment, gene expression of 12 m.o. 3xTg-AD mice *versus* 3 m.o. 3xTg-AD mice were not considered as such design would have produced results indicative of changes that can be indistinguishably depending on a mix of two factors (aging and the AD-like background).

The major aim of the study was to provide a better understanding of whether common genetic mechanisms are

[1]Functional Genetics Unit, Center of Excellence on Aging (CeSI), Chieti, Italy; [2]Department of Psychological Sciences, 'G. d'Annunzio' University, Chieti, Italy; [3]Department of Neuroscience and Imaging, 'G. d'Annunzio' University, Chieti, Italy; [4]Molecular Neurology Unit, Center of Excellence on Aging (CeSI), Chieti, Italy; [5]Departments of Neurology and Pharmacology, University of California-Irvine, Irvine, CA, USA and [6]Institute for Memory Impairments and Neurological Disorders, University of California-Irvine, Irvine, CA, USA
*Corresponding author: SL Sensi, Molecular Neurology Unit, Center of Excellence on Aging (CeSI), University 'G. d'Annunzio', Via dei Vestini, 31, Chieti 66100, Italy. Tel: +39 871 541544; Fax: +39 871 541542; E-mail: ssensi@uci.edu
[7]These authors contributed equally to this work.
Keywords: Alzheimer's disease; aging; microarray; inflammation; synaptic plasticity; mitochondria
Abbreviations: AD, Alzheimer's disease; m.o.a., months of age; Aβ, β-amyloid; WT, wild type; qRT-PCR, quantitative real-time PCR; ER, endoplasmic reticulum; LTP, long-term potentiation; NFT, neurofibrillary tangle; GABA, γ-aminobutyric acid; IPA, Ingenuity Pathway Analysis; SNP, single-nucleotide polimorphism; LOWESS, locally weighted scatterplot smoothing
Received 16.10.13; revised 12.12.13; accepted 07.1.14; Edited by A Verkhratsky

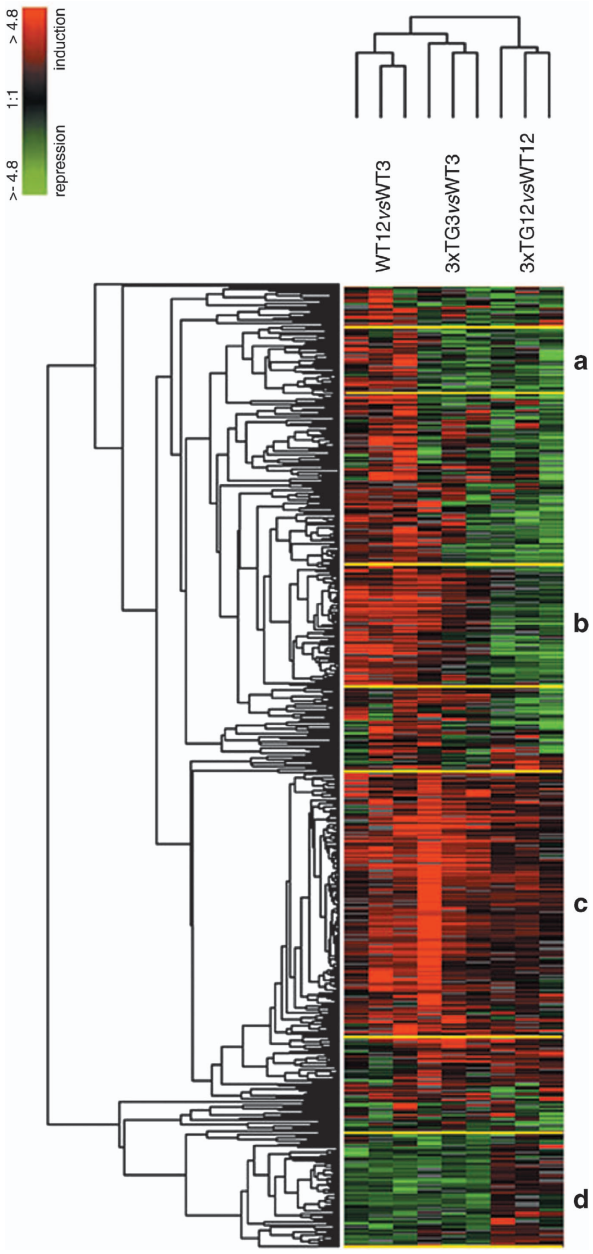

Figure 1 Unsupervised hierarchical clustering analysis. Transcripts that are clustered according to their expression values (log ratios) are shown. Each row indicates a transcript. The nine columns depict three replicates for each of the three experimental conditions listed on the top of the figure. Quantitative changes in gene expression are shown in colors. Red and green indicate upregulated and downregulated transcripts, respectively. Black indicates no changes in expression. Missing data points are shown in gray. (**a**) Cluster of 35 transcripts that were found downregulated in 3 m.o. 3xTg-AD *versus* 3 m.o. WT mice and 12 m.o. 3xTg-AD *versus* 12 m.o. WT mice. The same genes were instead upregulated in 12 m.o. WT *versus* 3 m.o. WT mice. (**b**) Cluster of 59 transcripts that were found to be specifically upregulated in 3 m.o. 3xTg-AD *versus* 3 m.o. WT mice and in 12 m.o. WT *versus* 3 m.o. WT mice. The same genes were instead downregulated in 12 m.o. 3xTg-AD *versus* 12 m.o. WT mice. (**c**) Cluster of 193 transcripts that were upregulated in all the experimental conditions (3 m.o. 3xTg-AD *versus* 3 m.o. WT mice and 12 m.o. 3xTg-AD *versus* 12 m.o. WT mice as well as in 12 m.o. WT *versus* 3 m.o. WT mice). (**d**) Cluster of 76 transcripts that were found downregulated in 3 m.o. 3xTg-AD *versus* 3 m.o. WT mice and in 12 m.o. WT *versus* 3 m.o. WT mice. The same genes were instead upregulated in 12 m.o. 3xTg-AD *versus* 12 m.o. WT mice

shared by aging and an AD-like background and whether overlapping pathogenic pathways can be identified in the two conditions.

Results

Cluster analysis of the investigated profiles revealed four different gene clusters (Supplementary Table 1), described in the following sections.

Cluster A. Cluster A consists of 35 transcripts that, compared with age-matched WT mice, were found downregulated in both 3 m.o. and 12 m.o. 3xTg-AD mice. The same gene set was found to be upregulated in 12 m.o. WT mice when compared with 3 m.o. WT (Figure 1a). The main biological functions associated with these genes are shown in Figure 2a and Table 1.

Cluster B. Cluster B consists of 59 transcripts that, compared with 3 m.o. WT mice, were upregulated in 3 m.o. 3xTg-AD mice and 12 m.o. WT mice. The same set was downregulated in 12 m.o. 3xTg-AD mice when compared with 12 m.o. WT mice (Figure 1b). These genes are implicated in key biological functions depicted in Figure 2b and Table 2.

Cluster C. Cluster C consists of 193 transcripts that, compared with age-matched WT mice, were upregulated in 3 m.o. and 12 m.o. 3xTg-AD mice. The same set was upregulated in 12 m.o. WT mice compared with 3 m.o. WT mice (Figure 1c). Functional analysis revealed that the overexpressed transcripts are associated with functions depicted in Figure 2c and Table 3.

Cluster D. Cluster D consists of 76 transcripts that, compared with 3 m.o. WT mice, were downregulated in 3 m.o. 3xTg-AD mice and 12 m.o. WT mice. These transcripts were upregulated in 12 m.o. 3xTg-AD mice when compared with 3 m.o. WT mice (Figure 1d). The main biological functions associated with these genes are provided in Figure 2d and Table 4.

TaqMan qRT-PCR: microarray data validation. In order to validate the microarray results, quantitative real-time PCR (qRT-PCR) analysis was performed on RNA extracted from the same hippocampal samples employed for microarray experiments. Analysis was performed on three upregulated genes (*BECN1*, *CST3*, and *GABRA5*) belonging to cluster C. In all cases, qRT-PCR confirmed the microarray results (Figure 3). Moreover, expression of the employed housekeeping gene (*GAPDH*) was stable among all the samples.

Interestingly, with the limitation and interpretative caution dictated by the low number of genes investigated by qRT-PCR ($n = 3$), we observed that young 3xTg-AD animals did already reach maximal expression that was not further changed, in a statistically significant manner, by aging (see 12 m.o. 3xTg-AD animals). On the contrary, in WT mice, these changes were occurring in an age-dependent way. Interestingly, young 3xTg-AD mice actually showed expression values that were higher compared with old WT mice.

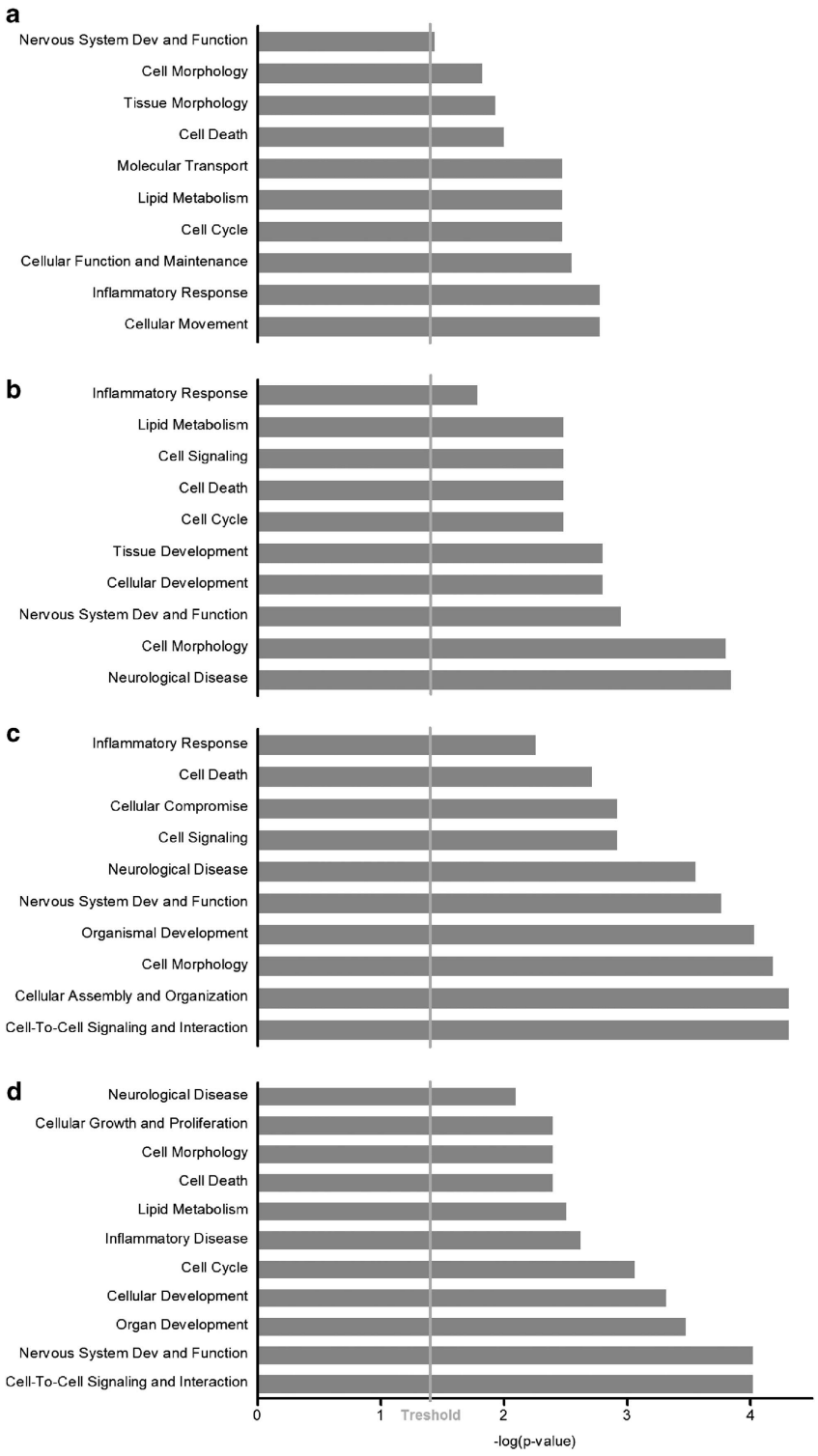

Figure 2 Biological functions as indicated by Ingenuity Pathway Analysis (IPA). Bar charts show results of IPA and indicate key biological functions modulated by genes selected in the four clusters described in Figure 1. (**a**) Cluster A, (**b**) cluster B, (**c**) cluster C, and (**d**) cluster D

Discussion

The main purpose of the study was to compare gene effects promoted by the pro-AD environment offered by the 3xTg-AD mice with those triggered, in WT mice, by senescence.

The most relevant finding is the identification of profile modifications detected in young 3xTg-AD mice that closely resemble those occurring upon physiological aging in WT animals, thereby suggesting that 3 m.o. 3xTg-AD mice

Table 1 IPA functional analysis of cluster A genes

Category	*P*-value	Molecules
Cellular movement	1,69E-03-4,63E-02	*GPR182, PEBP1, CPLX3, TMSB10/TMSB4X, HAS1*
Inflammatory response	1,69E-03-1,69E-03	*TMSB10/TMSB4X*
Cellular function and maintenance	2,84E-03-3,66E-02	*PEBP1, CPLX3, TMSB10/TMSB4X, CDC42EP2, HAS1*
Cell cycle	3,38E-03-8,43E-03	*CKAP2*
Lipid metabolism	3,38E-03-3,38E-03	*PEBP1*
Molecular transport	3,38E-03-3,66E-02	*PEBP1, CPLX3*
Cell death	1,01E-02-3,84E-02	*TMSB10/TMSB4X, CKAP2, DYSF, null*
Tissue morphology	1,18E-02-1,18E-02	*HAS1*
Cell morphology	1,51E-02-4,92E-02	*PEBP1, TMSB10/TMSB4X, ADCY6, VPS37C, HAS1*
Nervous system development and function	3,66E-02-3,66E-02	*CPLX3*

Table 2 IPA functional analysis of cluster B genes

Category	*P*-value	Molecules
Neurological disease	1,45E-04-4,55E-02	*CTR9, NEUROD1, CD200, YWHAE, HSPA1A/HSPA1B, EGR1, F7, SSR1, SCOC, SNAP25, MFAP2, CDH2, SOX9, RSPO2, PROCR, GABRA1*
Cell morphology	1,61E-04-4,87E-02	*NEUROD1, LDB3, YWHAE, PAM, HSPA1A/HSPA1B, EGR1, F7, OPHN1, SOX9, CDH2, NDUFS1, RSPO2, PROCR, GABRA1*
Nervous system development and function	1,14E-03-4,87E-02	*NEUROD1, CD200, YWHAE,RIT2, HSPA1A/HSPA1B, EGR1, ETV1, SNAP25, OPHN1, CDH2, SOX9, GABRA1, TACC1*
Cellular development	1,6E-03-4,43E-02	*NEUROD1, SOX9, HSPA1A/HSPA1B, RIT2, EGR1, RSPO2, F7, JAK3, SPRED2*
Tissue development	1,6E-03-4,75E-02	*NEUROD1, MFAP2, SOX9,CDH2, CD200, EGR1, F7, JAK3, CERCAM*
Cell cycle	3,32E-03-3,64E-02	*NEUROD1, SOX9, YWHAE, HSPA1A/HSPA1B, EGR1, JAK3*
Cell death	3,32E-03-4,95E-02	*NEUROD1, CD200, YWHAE, HSPA1A/HSPA1B, EGR1, F7, DNAJB9, DSG1, NDUFS1, CDH2, SOX9, UBA7, PROCR, JAK3, TACC1*
Cell signaling	3,32E-03-3,59E-02	*SOX9, CDH2, YWHAE, RIT2, IL10RB, F7, DOK3, SNAP25*
Lipid metabolism	3,32E-03-2,62E-02	*Rdh1 (*includes others*), F7*
Inflammatory response	1,65E-02-4,55E-02	*CD200, EGR1, F7, DOK3, YTHDF2*

undergo premature modulation of aging-related genes (Figure 4). For clarity and to improve readability of the section, we are discussing results of the three experimental conditions as follows:

- 3 m.o. 3xTg-AD *versus* 3 m.o. WT mice;
- 12 m.o. 3xTg-AD *versus* 12 m.o. WT mice;
- 12 m.o. WT *versus* 3 m.o. WT mice.

3 m.o. 3xTg-AD *versus* 3 m.o. WT mice. Comparisons between expression profile changes in young 3xTg-AD mice *versus* 3 m.o. WT mice revealed overexpression of several genes that are depicted in clusters B and C (Figures 1 and 4). These genes modulate several mechanisms (discussed below) that are serving a pathogenic role in AD.

$[Ca^{2+}]_i$ homeostasis. Deregulation of $[Ca^{2+}]_i$ is a key contributing factor for AD development and progression.[1,7] Perturbations in Ca^{2+} handling by the endoplasmic reticulum (ER) and mitochondria as well as impaired intra/extracellular cation exchange contribute to the neuronal dysfunction and degeneration occurring in brain aging and AD.[7] In cluster C, we found five genes involved in $[Ca^{2+}]_i$ homeostasis (*ATP2B1*, *CACNB4*, *RYR2*, *PKD2*, and *NDUFA9*). *ATP2B1* encodes for the plasma membrane Ca^{2+}-ATPase, a key system controlling high-capacitance/low-affinity Ca^{2+} extrusion, whereas *CACNB4* encodes for the voltage-dependent L-type calcium channel subunit β-4, a critical route for Ca^{2+} influx. Altered expression and functionality of these proteins correlate with deregulation of $[Ca^{2+}]_i$ as well as with development of a seizure-prone phenotype.[8] *CACNB4* is also associated with neuroprotective mechanisms in animal models of ischemic brain injury.[9] We also found changes in the expression of *RYR2. RYR2* encodes for the ryanodine receptor 2, a major system controlling Ca^{2+} release from the ER. *RYR2* overexpression found in 3xTg-AD mice is in line with previous findings supporting an important role for the ryanodine receptor type 2 that is promoting altered ER-Ca^{2+} release in presymptomatic 3xTg-AD mice.[10] This data set suggests a complex scenario in which enhanced $[Ca^{2+}]_i$ extrusion, mediated by *ATP2B1*, may compensate for impaired $[Ca^{2+}]_i$ buffering and excessive ER-Ca^{2+} release operated by *RYR2*.

Mitochondrial functioning. Alterations of mitochondrial functioning are crucial in physiological aging as well as in neurodegenerative conditions.[11] In clusters B and C, we found transcripts involved in the modulation of mitochondrial morphology and metabolism (*TRAK1 and Ndufs1* (cluster B); *Hax1*, *NDUFA9*, *GDAP1*, *KIF1B*, *HADBH*, *PGAM1*, *Ppia*, and *DNM1L* (cluster C)). *GDAP1* and *DNM1L* encode for proteins that promote mitochondrial fission; *PGAM1* encodes for an enzyme of the glycolytic pathway that is involved in mitochondrial-mediated protective effects against Aβ-induced cell death; *TRAK1* plays a critical role in axonal transport of mitochondria.[12–15] Finally, *Ndufs1* encodes for the NADH-ubiquinone oxidoreductase 75 kD, a subunit that regulates the activity of mitochondrial complex I. The early and sustained overexpression of transcripts involved in

Table 3 IPA functional analysis of cluster C genes

Category	*P*-value	Molecules
Cell-to-cell signaling and interaction	4,94E-05-2,9E-02	*B2M, APBA2, VCAM1, GABRA5, USP14, JAK1, NRP2, MAPK1, KIF1B, CACNB4, CRK, HES1 (*includes *EG:15205), VDAC3, App, IRF1 (*includes *EG:16362), SYBU, PMP22, DCC, RSU1*
Cellular assembly and organization	4,94E-05-2,9E-02	*B2M, APBA2, FHL1 (*includes *EG:14199), YWHAH, GPR12, MAPK1, KIF1B, HAX1, LPPR4, BOK, SNX3, CRK, BECN1, App, WASL, MYRIP, STARD13, DCC, MAP1LC3B, NRN1, VCAM1, NRP2, MED1 (*includes *EG:19014), RYR2, SEPT7, SMARCA5, YWHAZ, STK38L, MAPK9, GDAP1, VDAC3, TSG101, SYBU, PMP22, CETN3, Hmg1l1, HPRT1, DNM1L, ENC1*
Cell morphology	6,66E-05-3,45E-02	*B2M, APBA2, VCAM1, MAPK1, GPR12, NRP2, SEPT7, RYR2, STK38L, YWHAZ, CRK, GDAP1, HES1 (*includes *EG:15205), BECN1, VDAC3, App, TSG101, PMP22, Hmg1l1, STARD13, DCC, MAP1LC3B, DNM1L, NRN1*
Organismal development	9,48E-05-2,9E-02	*PAFAH1B2, VCAM1, JAK1, MAPK1, NRP2, MED1 (*includes *EG:19014), PKD2 (includes EG:18764), MAPK9, BECN1, App, H2AFZ, TSG101, WASL, Hmg1l1,CST3,TIMP2*
Nervous system development and function	1,75E-04-3,24E-02	*B2M, APBA2, USP14, GABRA5, GPR12, MAPK1, YWHAH, KIF1B, ITM2B, LPPR4, CRK, HES1 (includes EG:15205), App, SOX2, CST3, DCC, BPNT1, NRN1, HEY1, VCAM1, NRP2, MED1 (*includes *EG:19014), CACNB4, STK38L, YWHAZ, MAPK9, VDAC3, SYBU, PMP22, null, Hmg1l1, HPRT1, DNM1L, ENC1*
Neurological disease	2,83E-04-3,34E-02	*GABRA5, YWHAH, MAPK1, ATP6V1C1, ATP2B1, KIF1B, LPPR4, SLMAP, SOX2, PDHA1, TTBK2, PGAM1, GABRB1, PKIA, PGRMC1, G3BP2, IMPA1, HIAT1, YWHAZ, SPARCL1, HPRT1, CYC1, TMEM66, RSU1, ORC4, ENC1, B2M, APBA2, CA2, FHL1 (*includes *EG:14199), ITM2B, PPP1CB, BECN1, App, UNC79, TBCEL, FARSB, HADHB, TMEFF1, PPP3CB, CST3, STARD13, DCC, null, JKAMP, VCAM1, NRP2, SLC2A13, CACNB4, RYR2, MAPK9, GDAP1, KIFAP3 (*includes *EG:16579), HSPA12A, PMP22, AK5, null, DOCK8, PPIA, GLT25D2, DNM1L*
Cell signaling	1,23E-03-3,34E-02	*G3BP2, JAK1, MAPK1, ATP2B1, PKD2 (*includes *EG:18764), RYR2, CACNB4, STK38L, MAPK9, CRK, KIFAP3 (*includes *EG:16579), App, IRF1 (*includes *EG:16362), SOX2, CLK1, TRIM13, TTBK2, PPM1A, RSU1, TMEM9B, TIMP2*
Cellular compromise	1,23E-03-3E-02	*VCAM1, MAPK1, SEPT7, PGAM1, CRK, GDAP1, DNM1L, TSG101, App, IRF1 (*includes *EG:16362)*
Cell death	1,93E-03-3,45E-02	*PAFAH1B2, CA2, VCAM1, JAK1, MAPK1, KIF1B, MED1 (*includes *EG:19014), CUL1, YWHAZ, SMARCA5, MAPK9, BOK, HES1 (*includes *EG:15205), BECN1, KIFAP3 (*includes *EG:16579), TSG101, App, IRF1 (*includes *EG:16362), GNPTG, NT5C3, PMP22, AK5, Hmg1l1, DCC, PPM1A, TIMP2*
Inflammatory response	5,57E-03-3E-02	*VCAM1, JAK1, Hmg1l1, PPIA, PGAM1, App, IRF1 (*includes *EG:16362), TIMP2*

Table 4 IPA functional analysis of cluster D genes

Category	*P*-value	Molecules
Cell-to-cell signaling and interaction	9,74E-05-4,89E-02	*ST5, EPHB1, ARID1A, CCND3, BAIAP2, RGS4, STAT3*
Nervous system development and function	9,74E-05-4,99E-02	*ISLR2, NEUROD2, EPHB1, PRPF19, CCND3, ACTB, S100B, BAIAP2, PDE4A, RGS4, STAT3, DIO2, KLK8, RNF6, HIP1R*
Organ development	3,38E-04-4,59E-02	*EPHB1, CCND3, STAT3, DIO2*
Cellular development	4,87E-04-4,78E-02	*PRPF19, PA2G4, ELAVL3, PDE4A, RGS4, STAT3, DIO2, BIN1, GPC1, NEUROD2, LSMD1, CCND3, S100B, BAIAP2, BRD4, UBTF, TRRAP, SCAND1*
Cell cycle	8,76E-04-4,78E-02	*GPC1, MAP4, ARID1A, null, CCND3, PA2G4, EHMT2 (*includes *EG:10919), LAS1L, BRD4, STAT3, TRRAP*
Inflammatory disease	2,39E-03-3,47E-02	*CCND3, PDE4A, STAT3*
Lipid metabolism	3,14E-03-3,6E-02	*GPC1, MAP4, null, COTL1, HIP1R*
Cell death	4,07E-03-3,21E-02	*PRPF19, ARID1A, PA2G4, ACTB, PDE4A, RGS4, STAT3, CAPN10, KLK8, BIN1, ITPK1, GPC1, MAP4, LSMD1, CCND3, S100B, VCP, UBTF, TEX261*
Cell morphology	4,07E-03-4,39E-02	*ISLR2, MAP4, ACTB, BAIAP2, VCP, S100B, PDE4A, BRD4, RGS4, STAT3, TRRAP, RNF6*
Cellular growth and proliferation	4,07E-03-4,99E-02	*PRPF19, PA2G4, ACTB, RGS4, STAT3, NAA10, BIN1, GPC1, LSMD1, CCND3, EIF4A1, S100B, BRD4, PTPRS, LAS1L, UBTF, TRRAP*
Neurological disease	8,12E-03-3,21E-02	*S100B, STAT3*

mitochondrial fission (*GDAP1*, and *DNML1*) and neuroprotection (*PGAM1*) is in line with recent findings indicating that mitochondrial fission is neuroprotective through reduction of oxidative damages.[15]

Inflammatory response. Neuroinflammation is detrimental in brain aging and age-related cognitive decline.[16] The AD brain shows chronic, discrete, and microlocalized areas of inflammation as well as the appearance of activated microglia and reactive astrocytes in the vicinity of senile plaques.[1] Moreover, inflammatory-related genes and proteins (i.e., *CD33*, NLRP3) play a substantial role in Aβ-driven neurodegeneration and AD progression.[17,18] Cluster C revealed the presence of some transcripts (*APP*, *IRF1*, *PPIA*, *VCAM1*, *TIMP2*, *HMGB1L1*, *PGAM1*, and *JAK1*) that encode for proteins involved in the inflammatory response. It is noteworthy that in analogy with what was found for mitochondrial functioning, 3xTg-AD mice showed an early

activation of upstream (*IRF1*) and downstream (*JAK1*) proinflammatory transcripts.

Additional genes involved in the inflammatory response (*Hsp70*, *IL10 receptor*, and *CD200*) were also found (cluster D). However, these transcripts were downregulated (instead of upregulated when comparing 3 m.o. 3xTg-AD mice with 3 m.o. WT mice). Among these, *Hsp70* and *CD200* are known to play an anti-inflammatory role. Thus, the overexpression of inflammatory genes appears to be coupled with simultaneous decrease in the expression of anti-inflammatory transcripts, thereby suggesting an overall proinflammatory status.

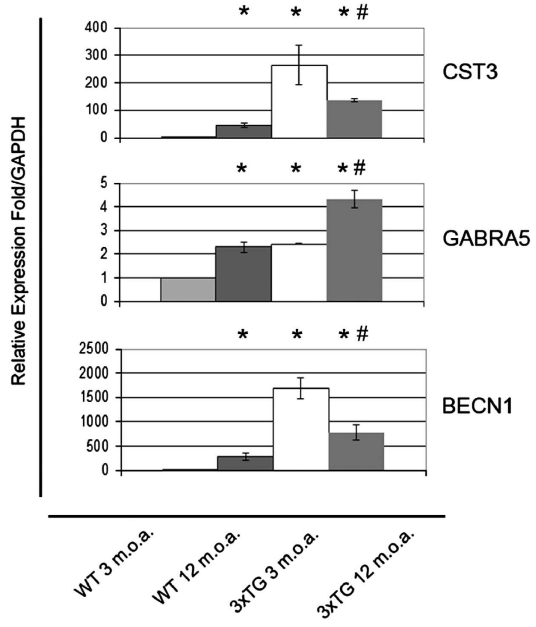

Figure 3 Validation of microarray gene expression data by qRT-PCR. Bar graph shows mRNA levels of *CST3*, *GABRA5*, and *BECN1* measured by real-time PCR in young and old WT mice and 3xTg-AD mice as well as in old WT mice and 3xTg-AD mice. Data are expressed as mean values of relative fold changes ± S.D. of three independent experiments performed in triplicate. The symbol '*' indicates that *CST3*, *GABRA5*, and *BECN1* are significantly upregulated when compared with gene expression in 3 m.o. WT mice ($P<0.05$). The symbol '#' indicates that *CST3*, *GABRA5*, and *BECN1* are significantly upregulated when compared with expression of these genes in 12 m.o. WT mice ($P<0.01$)

Dendrite formation, synaptic plasticity, and memory. Age- and AD-related cognitive decline is associated with synaptic dysfunction.[19] In that respect, we found overexpression of several transcripts (*CD200*, *Neurod1*, *SOX9*, *SNAP25*, *EGR1*, *OPHN1*, *ETV1*, *CDH2*, *GABRA1*, and *Spond1* (cluster B); *APBA2*, *APP*, *GABRA5*, *MAPK1*, *PMP22*, *SYBU*, *USP14*, *VDAC3*, *CST3*, *DCC*, *HES1*, *HEY1*, *HPRT1*, *SOX2*, *YWHAH*, *CRK*, *GPR12*, *HMGB1L1*, *STK38L*, and *VCAM1* (cluster C)) that are implicated in dendritic spine formation, modulation of synaptic functioning, and cognitive decline. Overexpression of transcripts encoding for proteins involved in synaptic activity and neurotransmission may be interpreted as a protective event against AD-related synaptic dysfunctions.

Overexpression of transcripts present in cluster C suggests a bimodal set of activities. One set of actions may counteract neuronal damage and promote protective effects aimed at maintaining cognitive abilities. For instance, *APBA2* is known to bind to *APP* and reduce Aβ production, thereby counteracting memory deficits and promoting long-term potentiation (LTP) in Tg AD mice.[20] Similarly, *CST3* upregulation is protective against the neurotoxic effects of Aβ oligomers and oxidative stress damage. This phenomenon has been reported in Tg AD models, in the brains of AD patients, and in those of elderly individuals.[21] The *GABRA5* transcript increase found in our 3xTg-AD mice lends support to the compensatory hypothesis as *GABRA5* has been reported to be downregulated with aging and this process has been linked to defective spatial memory performance.[22]

These protective actions are counteracted by the concurrent upregulation of transcripts that, on the contrary, are associated with neuronal dysfunction. This is the case of *APP* and *ERK2* transcripts. Given the aminoacidic composition of murine Aβ, murine *APP* is marginally involved in the formation of toxic Aβ species, but some studies have also proposed that the protein can favor *ERK1,2* activation, tau phosphorylation, and the formation of NFTs.[23] Chronic *ERK2* activation by Aβ oligomers can be detrimental as early and sustained *ERK2* stimulation has been shown to promote cognitive decline in AD mice[24] and induce neuronal toxicity through caspase-3 activation.[25]

	Young 3xTg-AD *vs.* Young WT	Old WT *vs.* Young WT	Old 3xTg-AD *vs.* Old WT	MAIN GENE FUNCTIONS	COMMENTS
Cluster A	↓	↑	↓	Dendritic spine formation Synaptic modulation Cognitive decline	Changes triggered by the pro-AD background occurring in young and old 3xTg-AD mice
Cluster B	↑	↑	↓	Mitochondrial functioning Inflammatory response	Changes occurring in old 3xTg-AD mice that might indicate defective response in counteracting disease progression
Cluster C	↑	↑	↑	Calcium homeostasis Mitochondrial functioning Inflammatory response	Changes occurring in all the three groups Of note, young 3xTg-AD mice show changes that are age-driven in WT mice
Cluster D	↓	↓	↑	Synaptic plasticity Neuronal proliferation Neuronal survival	Changes occurring in old 3xTg-AD mice that might indicate modulation of neuroprotective responses

Figure 4 Graphical synopsis of cluster analysis results. Synoptic view of all the transcriptome profiles that were found altered in the three experimental conditions. The main findings associated with observed gene expression changes are summarized. Note that, as depicted by the dark gray boxes, 3 m.o. 3xTg-AD *versus* 3 m.o. WT mice as well as 12 m.o. WT *versus* 3 m.o. WT mice show a similar pattern of expression changes in clusters B, C, and D. Also note that, only in the case of genes of cluster C, a common pattern of expression profiles is observed across all the three experimental conditions

It is interesting to note that in clusters A and D, we found downregulation of transcripts (*PEBP1* and *Complexin III* (cluster A) and *BIN*, *ACTB*, *BAIAP2*, *EphB*, *KLK8*, *ARD1*, *PDE4*, *Ehmt2*, *Neurod2*, *STAT3*, *S100B*, and *CCND3* (cluster D)) that are involved in dendritic spine formation, modulation of synaptic functioning, and cognitive decline. In this respect, *PEBP1* and *Complexin III* downregulation is associated with impaired cholinergic neurotransmission (*PEBP1*)[26] and synaptic transmission deficits (*Complexin III*),[27] the two mechanisms largely impaired in AD and in mild cognitive impairment.[28]

BAIAP2, *EphB1*, *BIN1*, and *KLK8* are involved in synaptic plasticity. *BAIAP2* (also known as *IRSp53*) modulates NMDA receptor-related synaptic transmission, LTP, as well as learning and memory. *BAIAP2* knockout mice show impaired spatial learning and novel object recognition.[29] Thus, *BAIAP2* downregulation might be involved in the development of cognitive deficits affecting this model that has been also shown to suffer from significant decrease in BDNF levels.[30] NMDAR deregulation has been associated with *EphB* (a family of ligand proteins) receptor deficits and linked to the appearance of neurological disorders including AD.[31] Still, in the set of synaptic plasticity-related genes that we found underexpressed, *KLK8* seems important as the gene is involved in brain development, neuronal plasticity, and stress response.[32] Thus, *KLK8* downregulation can favor aberrant CNS development. *S100B* is a calcium-binding protein released by astroglial cells. Compelling evidence indicates that transgenic animals, overexpressing S100B, show neuronal loss and increased expression of the pro-apoptotic protein clusterin, a protein that is increased in hippocampi and frontal cortices of AD patients.[33]

In summary, our findings suggest that 3xTg-AD mice not only show early modulation of transcripts that exert detrimental effects on synaptic functioning but also develop changes that counteract this impairment. The process appears to go on chronically as the same pattern is present in 12 m.o. 3xTg-AD mice.

Neuronal death, cell cycle, and autophagy. Aberrant expression of cell cycle- and autophagy-related molecules plays a pivotal role in the neuronal loss associated with AD and brain aging.[34,35] Our analysis revealed overexpression of a group of transcripts (*SPIN1*, *JAK3*, *Neurod1*, *SOX9*, *YWHAE*, *EGR1*, and *HSPA1A/HSPA1B* (cluster B); *Beclin-1*, *MAP1LC3-B*, *HADHB*, *AK5*, *CyC1*, *SIRT7* and *ENC1* (cluster C)) involved in autophagy, cell cycle, and cell death, thereby suggesting the potential activation of a complex network of neuronal death-related responses occurring in young 3xTg-AD mice.

Early *EGR1* upregulation has been reported in AD patients[36] and can contribute, along with other cell cycle-related genes, to NFT formation, a phenomenon that is also mediated by the increased expression of cell cycle proteins.[34,37] Furthermore, overexpression of *SPIN1* (a gene involved in cell cycle impairment) promotes chromosome instability, a process leading to cellular senescence and apoptosis.[38] *Sirt7*, a less investigated member of the sirtuin family, is a nuclear protein expressed in the brain with a cellular distribution and functions that are still unknown.[39] Experiments employing *Sirt7* knockout mice or *Sirt7*-overexpressing cells have indicated the antiproliferative role of the protein and suggested that *Sirt7* activity can improve tissue integrity in aging animals.[40]

Beclin-1 and *MAP1LC3-B* are two autophagy-related genes whose overexpression might counteract pathology development in 3 m.o. 3xTg-AD mice. This hypothesis is consistent with recent findings indicating that early induction of autophagy reduces cognitive decline in 3xTg-AD mice.[41,42] Autophagy, in fact, clears out damaged proteins that are prone to aggregation,[43] and the process can be neuroprotective by mediating the degradation of misfolded proteins.[44] Intriguingly, in AD, autophagy can play a dual role. On one hand, it is protective by promoting the removal of Aβ and tau aggregates and, on the other hand, autophagosomes are nevertheless sites of choice for accumulation and production of Aβ.[45–47]

Analysis of networks of genes involved in neuronal death also showed several transcripts that, compared with young WT mice, were found downregulated in young 3xTg-AD mice (*ARID1A*, *BRD4*, *CCND3*, *EHMT2*, *GPC1*, *LAS1L*, *MAP4*, *PA2G4*, *PTGES3*, *STAT3*, and *TRRAP* (cluster D)). Interestingly, aberrant expression of *CCND3* has been reported to be closely associated with AD-related neuronal death occurring in specific hippocampal regions.[48]

12 m.o. 3xTg-AD *versus* 12 m.o. WT mice. In order to evaluate how AD-like progression affects gene expression, we investigated profiles of 12 m.o. 3xTg-AD mice compared with 12 m.o. WT mice and matched this set of data with results of 3 m.o. 3xTg-AD mice that were compared with age-matched WT mice. The analysis revealed a similar overexpression of all transcripts of cluster C and downexpression of those of cluster A. Interesting differences appeared when analyzing transcripts belonging to clusters B and D (Figures 1 and 4).

Cluster B transcripts, overexpressed in young 3xTg-AD mice, were downregulated in 12 m.o. 3xTg-AD mice when compared with age-matched WT mice, a finding that supports the hypothesis that aged 3xTg-AD mice may show deficits in counteracting disease progression. Underexpression of many transcripts found in cluster B has been previously reported in several models of aging and AD as well as in AD patients. This is the case for *SNAP25* (encoding for a key protein involved in synaptic vesicle cycle and neurotransmission modulation),[49] *GABRA1* (encoding for a γ-aminobutyric acid (GABA) receptor subunit downregulated in AD brains),[50] *CDH2* (encoding for N-cadherin, whose deregulation triggers apoptotic pathway activation),[51] and *OPHN1* (encoding for a Rho-GTPase involved in controlling excitatory synapses maturation and plasticity).[52]

Cluster D transcripts, downexpressed in 3 m.o. 3xTg-AD, were instead overexpressed in aged 3xTg-AD. The upregulation of transcripts that are involved in the modulation of synaptic plasticity, neuronal proliferation, survival, differentiation, and regulation of cell division process might reflect a compensatory neuroprotective response (*BAIAP2*), although the net result suggests a more complex scenario (see, for instance, the role of *KLK8*). *BAIAP2* downregulation is related to altered synaptic plasticity as observed in

BAIAP2-deficient mice,[29] whereas its overexpression increases dendritic spine density and postsynaptic potentiation, ultimately enhancing cognition.[53] KLK8 deficiency promotes decreased synaptic plasticity, whereas, on the contrary, gain in *KLK8* mRNA levels has been observed in AD brains and equally associated with detrimental effects on hippocampal functioning.[54] Inhibition of *S100B* has positive effects on the Aβ load and gliosis observed in AD patients,[55] whereas *S100B* overexpression has been associated with exacerbation of AD clinical signs.[56,57] Finally, altered expression of cell cycle proteins (i.e., *CCND3*) in postmitotic neurons has been observed both in aging and in AD.

Collectively, over- and underexpression of the aforementioned transcripts confirm a pattern of responses in which some genes exert detrimental effects that are in line with the development of AD-like pathology. At the same time, other transcripts appear to counteract these effects. Interestingly, this process appears to progress chronically as a similar pattern has been reported in 3 m.o. and in 12 m.o. 3xTg-AD mice.

12 m.o. WT *versus* 3 m.o. WT mice. Finally, we compared expression profiles of 12 m.o. WT mice with 3 m.o. WT mice to analyze the effects of physiological aging.

Interestingly, changes driven by aging were largely overlapping with those observed in 3 m.o. 3xTg-AD mice when compared with 3 m.o. WT mice. We, in fact, observed overexpression of several transcripts belonging to clusters B and C and downregulation of a gene data set present in cluster D (Figures 1 and 4). The functional correlates of these changes have been discussed above.

Overall, these data support the hypothesis that the pro-AD environment offered by the 3xTg-AD mice accelerates and promotes early modifications of genes that are otherwise changed by aging in old WT mice. Moreover, comparison between 12 m.o. WT mice and age-matched 3xTg-AD mice showed expression changes that were similar only for genes belonging to cluster C.

Interestingly, Ingenuity Pathway Analysis (IPA) analysis of this cluster revealed transcripts (*HSPA12A*, *HIAT1*, *KIAA1409*, *NRP2*, *STARD13*, *UBB*, and *PKIA*) that genome-wide association studies have recently shown to be involved in AD-related single-nucleotide polimorphisms (SNPs) as well as transcripts (*APP*, *ATP6V1C1*, *BECN1*, *CST3*, *DCC*, *DNM1L*, *GABRA5*, *GABRB1*, *HIAT1*, *HSPA12A*, *KIAA1409*, *LPPR4*, *MAPK9*, *NRP2*, *PKIA*, *RYR2*, *STARD13*, *UBB*, and *YWHAZ*) that are closely related to AD development.

Finally, cluster A is the only one showing a unique behavior in 3xTg-AD mice, indicating changes that are specifically triggered by the pro-AD genetic background of the mice. It is intriguing to hypothesize that these genes have a functional role in AD progression and represent potential AD biomarkers. Among these, we observed a downregulation of *Homer3* and *Dysferlin*. Homer3 interacts with APP and inhibits Aβ production. Thus, *Homer3* downregulation can lead to enhanced Aβ production.[58] Accumulation in senile plaques of Dysferlin, a protein involved in membrane repair, leads to defective neuronal repair.[59] Thus, it is conceivable that the *Dysferlin* downregulation that we found in the 3xTg-AD mice can exert a similar detrimental effect.

Conclusions

With the limitation of any Tg-AD model, our data support the hypothesis that aging and AD share some mechanistic similarities. In our Tg-AD mouse, the pro-AD environment promotes and accelerates changes that, upon aging, are otherwise occurring in WT animals. Although the 3xTg-AD mice harbor three mutations that do not occur, at the same time, in AD human brains, this cumulative pro-AD background modulates in Tg mice the early on expression of genes, the so-called BioAge genes (associated with neuronal loss, glial activation, and lipid dysmetabolism) that are in humans biomarkers for brain aging and found prematurely expressed in AD patients.[60] The same accelerated expression of aging-related genes in AD has been recently reported in a study that analyzed AD brains,[61,62] thereby providing support for the heuristic value of 3xTg-AD mice as preclinical model of AD.

Our data support and integrate the age-based hypothesis for AD, a concept that postulates that aging is required to set in motion the AD-related pathogenic cascade. Our findings suggest the presence of a feed-forward mechanism by which pro-AD factors can promote aging-related gene profile changes, thereby boosting and accelerating the disease process. Furthermore, this is the first study that offers an extensive analysis of the transcriptomic profile of the 3xTg-AD model, one of the most comprehensive preclinical models of the disease. The novel set of AD-related genes found in our analysis will, likely, further studies investigating the molecular roadmap of the disease and its modulation by aging.

Materials and Methods

Animal models. All the procedures involving animals were approved by the institutional ethics committee (CeSI protocol no.: AD-301) and performed according to institutional guidelines and in compliance with national (DL no. 116, GU, Suppl. 40, 18 February 1992) and international laws and policies. The 3xTg-AD (harboring AD- related human mutation APP (Swe), PS1 (M146V), and tau (P301L) transgenes) female mice ($n=2$ at 3 m.o.a.; $n=2$ at 12 m.o.a.) and age-matched female control WT mice (129SV $\times$ C57BL/6, $n=2$ at 3 m.o.a.; $n=2$ at 12 m.o.a.) were kept in a temperature-controlled room at 25°C under a 12-h light/dark cycle and fed *ad libitum* with tap water and commercial chow. Mice at 3 or 12 m.o.a. were anesthetized and killed by decapitation, hippocampi excised, tissue transferred into RNA-later solution, and stored at -80°C for RNA processing.

Microarray analysis. Hippocampi were homogenized using a hand glass potter and total RNA extracted using the SVtotal RNA Isolation System kit following the manufacturer's instructions (Promega, Madison, WI, USA). RNA purity and quantity were estimated using an Agilent 8453 spectrophotometer (Agilent, Santa Clara, CA, USA). RNA samples were not pooled. Using the Amino Allyl MessageAmp II aRNA Amplification Kit (Ambion, Grand Island, NY, USA) RNA was amplified and fluorescently labeled with Cy3-Cy5 cyanins following the manufacturer's instructions. Labeled RNA was hybridized on high-density array containing 31 802 mouse transcripts (Mouse OneArray Whole Genome DNA microarray v1, Biosense, Milan, Italy). In order to increase the experimental homogeneity, we performed three replicates with a dye swap and each experiment contained RNA from hippocampi of young (3 m.o.a.) and old (12 m.o.a.) 3xTg-AD mice *versus* age-matched WT hippocampal RNA as control for a total of nine experiments. After hybridization, Cy3–Cy5 fluorescent signals were detected with a confocal laser scanner 'ScanArray Express' (Packard BioScience, Waltham, MA, USA) and analyzed with the 'ScanArray Express–MicroArray Analysis System 3.0' software (Perkin Elmer, Waltham, MA, USA). Raw data are stored in the GEO public database (accession number: GSE35210). Raw data were normalized using locally weighted scatterplot smoothing (LOWESS) algorithm. A transcript was considered differentially expressed when showing an absolute log-ratio value of $\geq \pm 0.5$, that is, 1.4 fold-change in transcript quantity. The transcript data set

was analyzed with gene clustering analysis using Cluster 3.0 (Stanford University Labs, Stanford, CA, USA). We evaluated only spots showing significant expression in at least 80% of the experiments. Data were centered to the mean of each mRNA and unsupervised average linkage hierarchical clustering of both the mRNAs and samples was performed using uncentered correlation metrics. Dendrograms and selected transcripts were visualized by employing TreeView software (Stanford University Labs). Gene biological functions were inferred using IPA software (Ingenuity Systems, Redwood City, CA, USA).

Real-time PCR. Microarray results were validated by performing qRT-PCR analysis on RNA extracted from hippocampi obtained from the same samples used for microarray analysis. Gene expression of three genes found upregulated by microarray (*BECN1*, *CST3*, and *GABRA5*) was evaluated. The *GAPDH* housekeeping gene was employed as internal control. qRT-PCR was performed in a total volume of 50 μl containing: 1 $\times$ TaqMan Universal PCR Master Mix, no AmpErase UNG, and 2 μl of cDNA using TaqMan assay on an Abi 7900HT Sequencing Detection System (Applied Biosystems, Paisley, UK). Transcript primers and probe sets employed were: *GAPDH*: primers FW: CTTTGTCAAGCT CATTTCCTGG, RW: TCTTGCTCAGTGTCCTTGC, probe CACCCTGTTGCTG TAGCCGTATTCA; *BECN1*: primers FW: GTACCGACTTGTTCCCTATGG, RW: ACACAGTCCAGAAAAGCTACC, probe: CCCCAGAACAGTATAACGGCAAC TCC; *CST3*: primers FW: CTGACTGTCCTTTCCATGACC, RW: TCCTTCTA GACTCAGCCCTTAG, probe: CCTTCCAGATCTACAGCGTGCCC; *GABRA5*: primers FW: GGGAATGGACAATGGAATGC, RW: TCTCATTGGTCTCGTCTTGTAC, probe: CATTTGCGAAAAGCCAAAGTGACCTGGA (Integrated DNA Technologies, Coralville, IA, USA). Real-time amplifications included 10 min at 95°C followed by 48 cycles of 15 s at 95°C and 1 min at 60°C. For each transcript, relative expression levels were normalized against the *GAPDH* gene. The $\Delta\Delta$Ct method was used to compare relative fold expression differences. One-way ANOVA was performed to assess statistically significant expression differences among the analyzed transcripts.

Conflict of Interest

The authors declare no conflict of interest.

1. Querfurth HW, LaFerla FM. Alzheimer's disease. *New Eng J Med* 2010; **362**: 329–344.
2. Krstic D, Knuesel I. Deciphering the mechanism underlying late-onset Alzheimer disease. *Nat Rev Neurol* 2013; **9**: 25–34.
3. Herrup K. Reimagining Alzheimer's disease–an age-based hypothesis. *J Neurosci* 2010; **30**: 16755–16762.
4. Tanzi RE. The genetics of Alzheimer disease. *Cold Spring Harb Perspect Med* 2012; **2**: 1–10.
5. Reddy PH, McWeeney S. Mapping cellular transcriptosomes in autopsied Alzheimer's disease subjects and relevant animal models. *Neurobiol Aging* 2006; **27**: 1060–1077.
6. Oddo S, Caccamo A, Shepherd JD, Murphy MP, Golde TE, Kayed R *et al.* Triple-transgenic model of Alzheimer's disease with plaques and tangles: intracellular Abeta and synaptic dysfunction. *Neuron* 2003; **39**: 409–421.
7. Corona C, Pensalfini A, Frazzini V, Sensi SL. New therapeutic targets in Alzheimer's disease: brain deregulation of calcium and zinc. *Cell Death Dis* 2011; **2**: e176.
8. Ketelaars SO, Gorter JA, Aronica E, Wadman WJ. Calcium extrusion protein expression in the hippocampal formation of chronic epileptic rats after kainate-induced status epilepticus. *Epilepsia* 2004; **45**: 1189–1201.
9. Jin K, Mao XO, Eshoo MW, Nagayama T, Minami M, Simon RP *et al.* Microarray analysis of hippocampal gene expression in global cerebral ischemia. *Ann Neurol* 2001; **50**: 93–103.
10. Chakroborty S, Kim J, Schneider C, Jacobson C, Molgo J, Stutzmann GE. Early presynaptic and postsynaptic calcium signaling abnormalities mask underlying synaptic depression in presymptomatic Alzheimer's disease mice. *J Neurosci* 2012; **32**: 8341–8353.
11. Lin MT, Beal MF. Mitochondrial dysfunction and oxidative stress in neurodegenerative diseases. *Nature* 2006; **443**: 787–795.
12. Pedrola L, Espert A, Wu X, Claramunt R, Shy ME, Palau F. GDAP1, the protein causing Charcot-Marie-Tooth disease type 4A, is expressed in neurons and is associated with mitochondria. *Hum Mol Genet* 2005; **14**: 1087–1094.
13. Miyamae Y, Han J, Sasaki K, Terakawa M, Isoda H, Shigemori H. 3,4,5-tri-O-caffeoylquinic acid inhibits amyloid beta-mediated cellular toxicity on SH-SY5Y cells through the upregulation of PGAM1 and G3PDH. *Cytotechnology* 2011; **63**: 191–200.
14. Brickley K, Stephenson FA. Trafficking kinesin protein (TRAK)-mediated transport of mitochondria in axons of hippocampal neurons. *J Biol Chem* 2011; **286**: 18079–18092.
15. Zhang Z, Kageyama Y, Sesaki H. Mitochondrial division prevents neurodegeneration. *Autophagy* 2012; **8**: 1531–1533.
16. Ownby RL. Neuroinflammation and cognitive aging. *Curr Psychiatry Rep* 2010; **12**: 39–45.
17. Heneka MT, Kummer MP, Stutz A, Delekate A, Schwartz S, Vieira-Saecker A *et al.* NLRP3 is activated in Alzheimer's disease and contributes to pathology in APP/PS1 mice. *Nature* 2013; **493**: 674–678.
18. Griciuc A, Serrano-Pozo A, Parrado AR, Lesinski AN, Asselin CN, Mullin K *et al.* Alzheimer's disease risk gene CD33 inhibits microglial uptake of amyloid beta. *Neuron* 2013; **78**: 631–643.
19. Selkoe DJ. Alzheimer's disease is a synaptic failure. *Science* 2002; **298**: 789–791.
20. Mitchell JC, Ariff BB, Yates DM, Lau KF, Perkinton MS, Rogelj B *et al.* X11beta rescues memory and long-term potentiation deficits in Alzheimer's disease APPswe Tg2576 mice. *Hum Mol Genet* 2009; **18**: 4492–4500.
21. Kaur G, Levy E. Cystatin C in Alzheimer's disease. *Front Mol Neurosci* 2012; **5**: 79.
22. Haberman RP, Quigley CK, Gallagher M. Characterization of CpG island DNA methylation of impairment-related genes in a rat model of cognitive aging. *Epigenetics* 2012; **7**: 1008–1019.
23. Nizzari M, Venezia V, Repetto E, Caorsi V, Magrassi R, Gagliani MC *et al.* Amyloid precursor protein and Presenilin1 interact with the adaptor GRB2 and modulate ERK 1,2 signaling. *J Biol Chem* 2007; **282**: 13833–13844.
24. Giovannini MG, Cerbai F, Bellucci A, Melani C, Grossi C, Bartolozzi C *et al.* Differential activation of mitogen-activated protein kinase signalling pathways in the hippocampus of CRND8 transgenic mouse, a model of Alzheimer's disease. *Neuroscience* 2008; **153**: 618–633.
25. Chong YH, Shin YJ, Lee EO, Kayed R, Glabe CG, Tenner AJ. ERK1/2 activation mediates Abeta oligomer-induced neurotoxicity *via* caspase-3 activation and tau cleavage in rat organotypic hippocampal slice cultures. *J Biol Chem* 2006; **281**: 20315–20325.
26. Maki M, Matsukawa N, Yuasa H, Otsuka Y, Yamamoto T, Akatsu H *et al.* Decreased expression of hippocampal cholinergic neurostimulating peptide precursor protein mRNA in the hippocampus in Alzheimer disease. *J Neuropathol Exp Neurol* 2002; **61**: 176–185.
27. Landgraf I, Muhlhans J, Dedek K, Reim K, Brandstatter JH, Ammermuller J. The absence of Complexin 3 and Complexin 4 differentially impacts the ON and OFF pathways in mouse retina. *Eur J Neurosci* 2012; **36**: 2470–2481.
28. Haense C, Kalbe E, Herholz K, Hohmann C, Neumaier B, Krais R *et al.* Cholinergic system function and cognition in mild cognitive impairment. *Neurobiol Aging* 2012; **33**: 867–877.
29. Kim MH, Choi J, Yang J, Chung W, Kim JH, Paik SK *et al.* Enhanced NMDA receptor-mediated synaptic transmission, enhanced long-term potentiation, and impaired learning and memory in mice lacking IRSp53. *J Neurosci* 2009; **29**: 1586–1595.
30. Corona C, Masciopinto F, Silvestri E, Viscovo AD, Lattanzio R, Sorda RL *et al.* Dietary zinc supplementation of 3xTg-AD mice increases BDNF levels and prevents cognitive deficits as well as mitochondrial dysfunction. *Cell Death Dis* 2010; **1**: e91.
31. Sheffler-Collins SI, Dalva MB. EphBs: an integral link between synaptic function and synaptopathies. *Trends Neurosci* 2012; **35**: 293–304.
32. Yousef GM, Kishi T, Diamandis EP. Role of kallikrein enzymes in the central nervous system. *Clin Chim Acta* 2003; **329**: 1–8.
33. Shapiro LA, Bialowas-McGoey LA, Whitaker-Azmitia PM. Effects of S100B on serotonergic plasticity and neuroinflammation in the hippocampus in Down syndrome and Alzheimer's disease: studies in an S100B overexpressing mouse model. *Cardiovasc Psychiatry Neurol* 2010; **2010**: 1–13.
34. Bowser R, Smith MA. Cell cycle proteins in Alzheimer's disease: plenty of wheels but no cycle. *J Alzheimers Dis* 2002; **4**: 249–254.
35. Nixon RA, Yang DS. Autophagy and neuronal cell death in neurological disorders. *Cold Spring Harb Perspect Biol* 2012; **4**: 10.
36. Gomez Ravetti M, Rosso OA, Berretta R, Moscato P. Uncovering molecular biomarkers that correlate cognitive decline with the changes of hippocampus' gene expression profiles in Alzheimer's disease. *PLoS One* 2010; **5**: e10153.
37. Lu Y, Li T, Qureshi HY, Han D, Paudel HK. Early growth response 1 (Egr-1) regulates phosphorylation of microtubule-associated protein tau in mammalian brain. *J Biol Chem* 2011; **286**: 20569–20581.
38. Yuan H, Zhang P, Qin L, Chen L, Shi S, Lu Y *et al.* Overexpression of SPINDLIN1 induces cellular senescence, multinucleation and apoptosis. *Gene* 2008; **410**: 67–74.
39. Schwer B, Schumacher B, Lombard DB, Xiao C, Kurtev MV, Gao J *et al.* Neural sirtuin 6 (Sirt6) ablation attenuates somatic growth and causes obesity. *Proc Natl Acad Sci USA* 2010; **107**: 21790–21794.
40. Vakhrusheva O, Braeuer D, Liu Z, Braun T, Bober E. Sirt7-dependent inhibition of cell growth and proliferation might be instrumental to mediate tissue integrity during aging. *J Physiol Pharmacol* 2008; **59**(Suppl 9): 201–212.
41. Majumder S, Richardson A, Strong R, Oddo S. Inducing autophagy by rapamycin before, but not after, the formation of plaques and tangles ameliorates cognitive deficits. *PLoS One* 2011; **6**: e25416.
42. Khandelwal PJ, Herman AM, Hoe HS, Rebeck GW, Moussa CE. Parkin mediates beclin-dependent autophagic clearance of defective mitochondria and ubiquitinated Abeta in AD models. *Hum Mol Genet* 2011; **20**: 2091–2102.
43. Ma Q, Qiang J, Gu P, Wang Y, Geng Y, Wang M. Age-related autophagy alterations in the brain of senescence accelerated mouse prone 8 (SAMP8) mice. *Exp Gerontol* 2011; **46**: 533–541.
44. Metcalf DJ, Garcia-Arencibia M, Hochfeld WE, Rubinsztein DC. Autophagy and misfolded proteins in neurodegeneration. *Exp Neurol* 2012; **238**: 22–28.
45. Yu WH, Cuervo AM, Kumar A, Peterhoff CM, Schmidt SD, Lee JH *et al.* Macroautophagy–a novel Beta-amyloid peptide-generating pathway activated in Alzheimer's disease. *J Cell Biol* 2005; **171**: 87–98.
46. Levine B, Kroemer G. Autophagy in the pathogenesis of disease. *Cell* 2008; **132**: 27–42.

47. Tung YT, Wang BJ, Hu MK, Hsu WM, Lee H, Huang WP *et al.* Autophagy: a double-edged sword in Alzheimer's disease. *J Biosci* 2012; **37**: 157–165.
48. Busser J, Geldmacher DS, Herrup K. Ectopic cell cycle proteins predict the sites of neuronal cell death in Alzheimer's disease brain. *J Neurosci* 1998; **18**: 2801–2807.
49. VanGuilder HD, Yan H, Farley JA, Sonntag WE, Freeman WM. Aging alters the expression of neurotransmission-regulating proteins in the hippocampal synaptoproteome. *J Neurochem* 2010; **113**: 1577–1588.
50. Limon A, Reyes-Ruiz JM, Miledi R. Loss of functional GABA(A) receptors in the Alzheimer diseased brain. *Proc Natl Acad Sci USA* 2012; **109**: 10071–10076.
51. Ando K, Uemura K, Kuzuya A, Maesako M, Asada-Utsugi M, Kubota M *et al.* N-cadherin regulates p38 MAPK signaling via association with JNK-associated leucine zipper protein: implications for neurodegeneration in Alzheimer disease. *J Biol Chem* 2011; **286**: 7619–7628.
52. Nadif Kasri N, Nakano-Kobayashi A, Malinow R, Li B, Van Aelst L. The Rho-linked mental retardation protein oligophrenin-1 controls synapse maturation and plasticity by stabilizing AMPA receptors. *Genes Dev* 2009; **23**: 1289–1302.
53. Choi J, Ko J, Racz B, Burette A, Lee JR, Kim S *et al.* Regulation of dendritic spine morphogenesis by insulin receptor substrate 53, a downstream effector of Rac1 and Cdc42 small GTPases. *J Neurosci* 2005; **25**: 869–879.
54. Shimizu-Okabe C, Yousef GM, Diamandis EP, Yoshida S, Shiosaka S, Fahnestock M. Expression of the kallikrein gene family in normal and Alzheimer's disease brain. *Neuroreport* 2001; **12**: 2747–2751.
55. Mori T, Koyama N, Arendash GW, Horikoshi-Sakuraba Y, Tan J, Town T. Overexpression of human S100B exacerbates cerebral amyloidosis and gliosis in the Tg2576 mouse model of Alzheimer's disease. *Glia* 2010; **58**: 300–314.
56. Bialowas-McGoey LA, Lesicka A, Whitaker-Azmitia PM. Vitamin E increases S100B-mediated microglial activation in an S100B-overexpressing mouse model of pathological aging. *Glia* 2008; **56**: 1780–1790.
57. Michetti F, Corvino V, Geloso MC, Lattanzi W, Bernardini C, Serpero L *et al.* The S100B protein in biological fluids: more than a lifelong biomarker of brain distress. *J Neurochem* 2012; **120**: 644–659.
58. Parisiadou L, Bethani I, Michaki V, Krousti K, Rapti G, Efthimiopoulos S. Homer2 and Homer3 interact with amyloid precursor protein and inhibit Abeta production. *Neurobiol Dis* 2008; **30**: 353–364.
59. Galvin JE, Palamand D, Strider J, Milone M, Pestronk A. The muscle protein dysferlin accumulates in the Alzheimer brain. *Acta Neuropathol* 2006; **112**: 665–671.
60. Podtelezhnikov AA, Tanis KQ, Nebozhyn M, Ray WJ, Stone DJ, Loboda AP. Molecular insights into the pathogenesis of Alzheimer's disease and its relationship to normal aging. *PLoS One* 2011; **6**: e29610.
61. Saetre P, Jazin E, Emilsson L. Age-related changes in gene expression are accelerated in Alzheimer's disease. *Synapse* 2011; **65**: 971–974.
62. Cooper-Knock J, Kirby J, Ferraiuolo L, Heath PR, Rattray M, Shaw PJ. Gene expression profiling in human neurodegenerative disease. *Nat Rev Neurol* 2012; **8**: 518–530.

Supplementary Information accompanies this paper on Cell Death and Disease website (http://www.nature.com/cddis)